Signal Processing Research (SPR) Volume 4, 2015
doi: 10.14355/spr.2015.04.007

Computation of Satellite Yaw Angular Velocity for Relative Radiometric Calibration

Li Haichao*[1], Man Yiyun[2]

Qian Xuesen Laboratory of Space Technology, China Academy of Space Technology, 100094, Beijing, China

*[1]lihaichao2000@163.com; [2]man_yy@163.com

Abstract

The purpose of relative radiometric calibration is to eliminate the strip phenomenon on the image. A new method with all detectors viewing the same scene is carried out. This paper provides the modeling and computation of satellite Yaw Angular Velocity(YAV) based on all the CCD detectors imaging the same region. The space coordinate transform process from object point on the earth to image point in the focal plane is found. Furthermore, the calculation method and process of YAV for satellite CCD camera imaging the same scene is given. Computation results indicate that the ground trajectory interval width is less than one pixel near the equator, and about four pixels below 35 degrees during calibration process more than 30 seconds imaging for 30000 detectors imaging the same scene.

Keywords

Remote Sensing Satellite; Linear CCD; Relative Radiometric Calibration; Yaw Angular Velocity; The Same Scene Imaging

Introduction

At present, the optical remote sensing satellite mainly uses the linear CCD camera to obtain the remote sensing images. Due to the non-uniformity noise and dark current noise presented in the CCD detector, the obvious strip exists in the raw images obtained from the linear CCD (Corsini,2000). Relative radiometric calibration is used to determine the normalization correction coefficient in order to remove strip noise.

The arrays are slightly tilted so as to reduce the effect of distortion during operation in TDI mode. For example, the focal plane of Pleiades-HR is composed of five slightly tilted TDI arrays (Greslou,2012). At present, laboratory integrating sphere calibration method can be satisfied with the image correction before satellite launching. However, the calibration coefficients of the camera will change with satellite launch, aging (Markham,1998). The methods of histogram matching (Horn,1979), moment matching (Gadallah,2000) are mainly based on the assumption that each sensor is exposed to scene radiance with approximately the same probability distribution. The side-slither maneuver method is a new method, which involves yawing the satellite 90°(Cody,2011). This paper provides the computation method of satellite YAV for slightly tilted CCD viewing the same scene, based on the establishment of strict conversion from geographic coordinate to focal plane coordinate.

Coordinates Transformation for Satellite Squint Imaging

There are seven coordinates involved in the coordinate transformation from object point on the earth to image point in the focal plane. They are defined as follows:

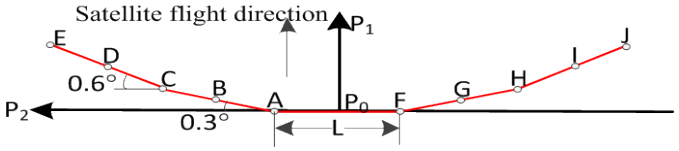

FIG. 1 FOCAL PLANE SKETCH MAP

Focal Plane Coordinate System (FPCS): P0-P1P2P3

Origin P_0 is center of CCD arrays, and P_1, P_2, P_3 are parallel to roll, pitch and yaw axes, respectively. As shown in FIG.1, CCD camera is in conventional imaging mode, the tilted five CCD arrays are closer to being perpendicular to the satellite flight direction, and the incline angle with each other is 0.3°. When on-orbit running, considered

influence of lens distortion and earth curvature, CCD arrays should be carried with geometry calibration for obtaining the actual model. Here the five CCD arrays model is fitted with circle. Poins A,B,C,…,J are the end and mid points of five arrays analyzed in after experiments.

Geographical Coordinate System (GCS): G0-G1G2G3

G_0 is the origin of GCS, and also the corresponding ground point of P_0. G_1 is parallel to flight direction. G_3 is pointing to zenith. G_2 is perpendicular to G_1G_3 plane.

Inertial Coordinate System (ICS):O-I1I2I3

Origin O is at geocenter, I_2 points to north pole, I_3 pointing satellite orbit plane and the equatorial plane intersection, I_1 is perpendicular to I_2 and I_3.

Earth Fixed Coordinate System (EFCS):O-E1E2E3

E_2 points to north pole. It is in inertial space, around the counter clockwise direction with velocity ω.

Orbit Coordinate System (OCS):B0-B1B2B3

Origin B_0 is located on the orbit, and B_1 points to the track direction, B_2 is perpendicular to the surface of the satellite orbit, B_3 towards the zenith.

Body Coordinate System (BCS):S0-S1S2S3

Origin is the same as that of OCS. The three axial positions of ϕ ,θ,ψ mean that of BCS in OCS.

Camera Coordinate System (CCS):C0-C1C2C3

Without installation error, CCS is the same as BCS.

This proposed transformation model takes into accout not only ϕ ,θ,ψ equal to zero, but also unequal to zero, which is different with Ref.(Wang,2005) only considering nadir point. Transformation from object point in GCS to image point in FPCS is established:

Following the translation procedures and relationship shown in FIG.2 and FIG.3, the transformation from GCS to FPCS is expressed as the following formula (1):

$$
\begin{bmatrix} P_1 \\ P_2 \\ P_3 \\ 1 \end{bmatrix} = \begin{bmatrix} f/(H-h) & 0 & 0 & 0 \\ 0 & f/(H-h) & 0 & 0 \\ 0 & 0 & f/(H-h) & 0 \\ 0 & 0 & 0 & f \end{bmatrix} \begin{bmatrix} \cos\psi & \sin\psi & 0 & 0 \\ -\sin\psi & \cos\psi & 0 & 0 \\ 0 & 0 & 1 & 0 \\ 0 & 0 & 0 & 1 \end{bmatrix} \begin{bmatrix} \cos\theta & 0 & -\sin\theta & 0 \\ 0 & 1 & 0 & 0 \\ \sin\theta & 0 & \cos\theta & 0 \\ 0 & 0 & 0 & 1 \end{bmatrix} \begin{bmatrix} 1 & 0 & 0 & 0 \\ 0 & \cos\varphi & \sin\varphi & 0 \\ 0 & -\sin\varphi & \cos\varphi & 0 \\ 0 & 0 & 0 & 1 \end{bmatrix}
$$

$$
\begin{bmatrix} 1 & 0 & 0 & 0 \\ 0 & 1 & 0 & 0 \\ 0 & 0 & 1 & -(R+H) \\ 0 & 0 & 0 & 1 \end{bmatrix} \begin{bmatrix} \cos\gamma & 0 & -\sin\gamma & 0 \\ 0 & 1 & 0 & 0 \\ \sin\gamma & 0 & \cos\gamma & 0 \\ 0 & 0 & 0 & 1 \end{bmatrix} \begin{bmatrix} \cos i_0 & \sin i_0 & 0 & 0 \\ -\sin i_0 & \cos i_0 & 0 & 0 \\ 0 & 0 & 1 & 0 \\ 0 & 0 & 0 & 1 \end{bmatrix} \begin{bmatrix} \cos\omega t & 0 & \sin\omega t & 0 \\ 0 & 1 & 0 & 0 \\ -\sin\omega t & 0 & \cos\omega t & 0 \\ 0 & 0 & 0 & 1 \end{bmatrix} \begin{bmatrix} \cos i_0 & -\sin i_0 & 0 & 0 \\ \sin i_0 & \cos i_0 & 0 & 0 \\ 0 & 0 & 1 & 0 \\ 0 & 0 & 0 & 1 \end{bmatrix}
$$

$$
\begin{bmatrix} \cos\gamma_0 & 0 & \sin\gamma_0 & 0 \\ 0 & 1 & 0 & 0 \\ -\sin\gamma_0 & 0 & \cos\gamma_0 & 0 \\ 0 & 0 & 0 & 1 \end{bmatrix} \begin{bmatrix} 1 & 0 & 0 & 0 \\ 0 & \cos\angle K_0OK_1 & \sin\angle K_0OK_1 & 0 \\ 0 & -\sin\angle K_0OK_1 & \cos\angle K_0OK_1 & 0 \\ 0 & 0 & 0 & 1 \end{bmatrix} \begin{bmatrix} \cos\angle K_1OG_0 & 0 & -\sin\angle K_1OG_0 & 0 \\ 0 & 1 & 0 & 0 \\ \sin\angle K_1OG_0 & 0 & \cos\angle K_1OG_0 & 0 \\ 0 & 0 & 0 & 1 \end{bmatrix} \begin{bmatrix} 1 & 0 & 0 & 0 \\ 0 & 1 & 0 & 0 \\ 0 & 0 & 1 & (R+h) \\ 0 & 0 & 0 & 1 \end{bmatrix} \begin{bmatrix} G_1 \\ G_2 \\ 0 \\ 1 \end{bmatrix} \tag{1}
$$

Where, R is earth radius, H is satellite height, h is object height, i_0 is orbit incline angle, γ is geocentric angle between satellite and ascending node, $\gamma=\gamma_0+\Omega t$, Ω is satellite angle velocity, ω is earth rotation velocity, $\psi=\psi_0+d\psi t$, $\theta=\theta_0+d\theta t$, $\phi=\phi_0+d\phi t$, ψ_0, θ_0, ϕ_0 are initial angles, and $d\psi$,$d\theta$,$d\phi$ are velocity. $\angle K_0OK_1$ and $\angle K_1OG_0$ are geocentric angles with squint imaging mode, shown in FIG.3 (right), which are computed:

In ΔB_0OK_1, $\angle K_0OK_1=\arcsin\left[(R+H)\sin\varphi/R\right]-\varphi$, $B_0K_1=\sqrt{(R+H)^2+R^2-2\cdot(R+H)\cdot R\cdot\cos\angle K_0OK_1}$

In ΔB_0OG_0, $\angle OB_0G_0 = \arccos(\cos\theta\cos\varphi)$, $\angle B_0OG_0 = \arcsin\left(\frac{R+H}{R}\sin\angle OB_0G_0\right) - \angle OB_0G_0$,

$$B_0G_0 = \sqrt{(R+H)^2 + R^2 - 2\cdot(R+H)\cdot R\cdot\cos\angle B_0OG_0}$$

In $\Delta B_0K_1G_0$, $K_1G_0 = \sqrt{B_0K_1{}^2 + B_0G_0{}^2 - 2\cdot B_0K_1\cdot B_0G_0\cdot\cos\theta}$, Therefore, in ΔK_1OG_0, $\angle K_1OG_0 = 2\cdot\arcsin\frac{K_1G_0}{2R}$

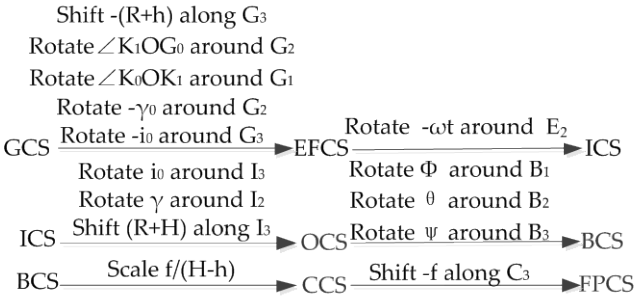

FIG. 2PROCEDURES OF TRANSFORMATION

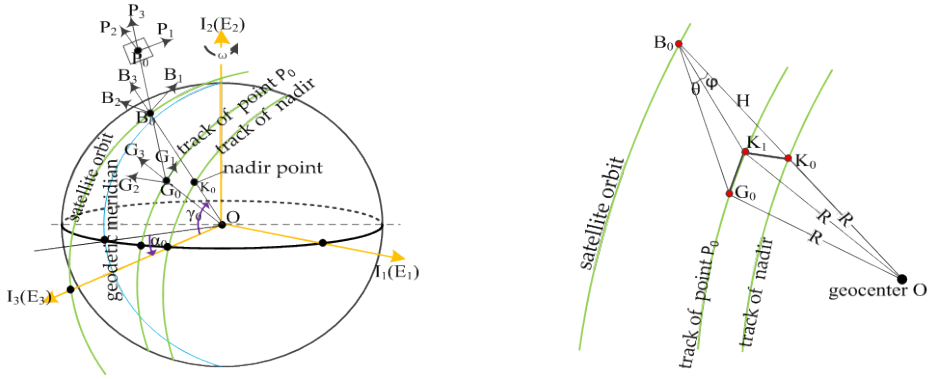

FIG. 3 CONVERSION FROM GCS TO FCS (LEFT:RELATION, RIGHT: GEOCENTRIC ANGLE CAUSED BY SQUINT IMAGING)

Computation of Satellite YAV

As shown in FIG.4, in orbit position A, satellite is with conventional imaging mode, according to the formula (1) the drift angle β_0 can be calculated. And then the satellite yaw angle is rotated 90-β_0 degrees clockwise direction, and in orbit position B, satellite is with the relative radiometric calibration mode. Where the β_0 is to remove influence of earth's rotation. And focal plane for calibration mode is shown in FIG.4(RIGHT).

However, when on-orbit calibration imaging, due to the slightly tilted of CCD arrays, it is needed to constantly adjust yaw angle. To make all the detectors imaging the same region, they must be strictly through the same point in the natural scene, and all detectors along the same trajectory ground, so a large amount of data all the detectors imaging the same region can be obtained. YAV can be computed as following steps:

1) As shown in FIG.5, suppose the start time t_0 of performing relative calibration is imaging zero. When the corresponding FPCS with origin P_0 is known as the original FPCS (OFPCS), and the corresponding GCS with origin G_0 is known as the original GCS (OGCS).

2) OFPCS shifts along satellite flight direction with CCD size d_e, simultaneously OFPCS rotates aroung origin P_0 with certain YAV. After time t_1, $t_1=n_1*t_e$, OFPCS will arrive at new point P_0', which is the origin of new FPCS (NFPCS) P_0'-$P_1'P_2'P_3'$.

Where t_e is the integral time of CCD, n_1 is the moving pixel number of FPCS, therefore coordinate value of P_0' in NFPCS can be computed with $p_{10}'=n_1d_e\sin\beta_0$, $p_{20}'=n_1d_e\cos\beta_0$. According to formula (1), the corresponding coordinate value of P_0' in OGCS can be calculated, defined as $G_0'(g_{10}',g_{20}',0)$.

3) According to the condition of all detectors viewing the same ground scene, suppose point N in OFPCS and point

M′ in NFPCS pointing to the same ground point, as shown in FIG.5. Set the coordinates of point N in OGCS is expressed as $P_N(p_{1N},p_{2N},0)$, and compute corresponding geographical coordinates $G_N(g_{1N},g_{2N},0)$ in OGCS according to formula (1).

Suppose coordinates of point M′ in NFPCS is $P_{M'\_new}(p_{1M'\_new},p_{2M'\_new},0)$. The relationship of M′ and N in FPCS is $p_{2M'\_new}=(p_{2N}-p_{20}'/\cos\beta_0)$, likewise, the corresponding coordinates of M′ in NGCS is computed, expressed as $G_{M'\_new}(g_{1M'\_new},g_{2M'\_new},0)$.

4) Then , with the condition of viewing the same scene, there is $g_{2M'\_new}+g_{20}'$ equals to g_{2N}. Get the complex trigonometric function equation, and the satellite YAV can be calculated.

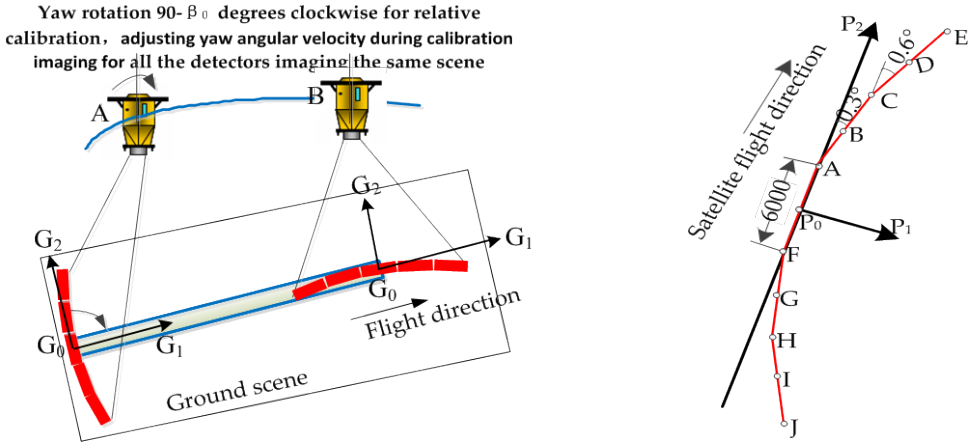

FIG. 4 ON-ORBIT CALIBRATION (LEFT:YAW ROTATION FOR CALIBRAITON, RIGHT: FOCAL PLANE WHEN CALIBRATION)

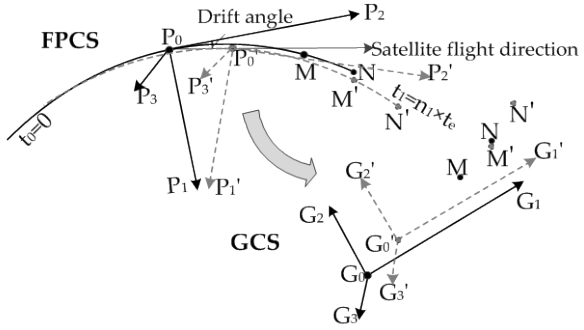

FIG. 5 DIAGRAM OF SATELLITE YAV COMPUTATION FOR ALL CCD DETECTORS VIEWING THE SAME SCENE

Experiments and Analysis

In this paper, experimental simulation parameters are: per linear CCD length 6000 pixels with 5 pieces, focal length 2600mm, integration time 362.59μs. Satellite orbital height H 645.338km, earth radius R 6378.137km, satellite orbit period 98 min, orbit incline angle 98°.

FIG.6 shows trajectories of 11 detectors (P_0, A, B, C, …, I, and J) in 5 CCD arrays, as shown in FIG.4 (RIGHT), within about 32 seconds, where, at 0º latitude, YAV adjusting period equals to 0.36s. The different color curves are the trajectories. As distortion makes the projection of the detector unstraight, the trajectories are also curved. The rectangular box area with red dashed line is common area with all 11 detectors passed through, where the maximum mean width within the region is 2.157m. In order to see clearly this thickness, the trajectories on the ground are enlarged, shown in FIG.6(b). FIG.6 (c) is YAV curve, which is first increased from -0.06761°/s to -0.06617°/s and then decreased to -0.06747°/s.

Table 1 gives the mean width of trajectories with YAV adjusting period all equals to 0.36s at different latitudes and roll angles. It can be seen that near the equator, the width is very narrow, such as width is 2.157m at 0º, and 1.378m at 5º. The ground track accuracy is better than 1 pixel for 2.5m resolution satellite. With the increasing of latitude, the ground track width is wider and wider. And until 50 degrees, the ground width has reached 15m (6 pixels).

With roll angle increasing, the width near equator is the most obvious changing, such as from roll angle from 0º to 40º, width changing from 2.157m to 22.287m.

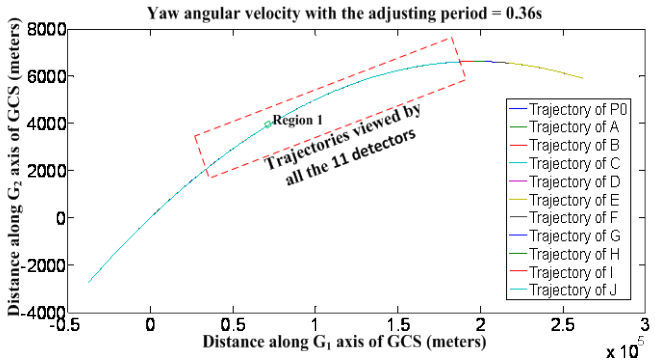

(a)THE WHOLE TRAJECTORIES

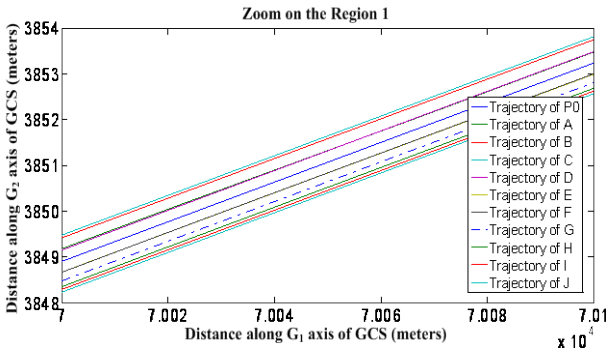

(b) ZOOM ON REGION 1

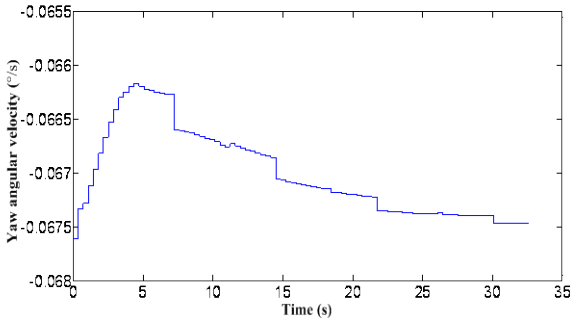

(c) CORRESPONDING YAV

FIG.6 TRAJECTORIES OF 11 DETECTORS IN 5 ARRAYS (LATITUDE=ZERO DEGREE, YAV ADJUSTING PERIOD=0.36S)

TABLE 1 TRAJECTORY WIDTH AT DIFFERENT LATITUDES AND ROLL ANGLES (METER)

Latitude(°) / Roll angle(°)	0	5	10	15	20	25	30	35	40	45	50
0	2.157	1.378	3.215	3.806	5.634	7.511	9.828	11.662	12.918	13.697	15.054
5	2.163	1.853	3.578	3.906	5.766	7.602	9.265	11.667	12.803	14.183	15.329
10	2.668	2.602	4.093	4.075	6.049	7.56	9.386	10.827	12.246	13.619	14.971
15	4.069	3.718	4.834	4.219	6.305	7.569	9.866	11.285	12.57	13.743	14.989
20	6.258	5.269	5.855	4.466	6.502	7.552	9.3205	10.644	12.147	13.54	14.791
25	7.858	7.415	7.236	4.794	6.339	7.687	8.868	10.458	12.026	13.697	15.727
30	10.747	10.355	9.092	5.183	5.899	7.951	8.873	10.573	12.42	14.164	16.14
35	15.127	13.349	11.568	5.814	5.673	8.039	8.94	10.964	13.69	16.885	19.9
40	22.287	17.739	14.929	6.982	5.684	8.3	9.08	12.416	16.127	20.609	26.65

Conclusion

To view the same scene for the relative radiometric calibration of multi tilted CCD arrays, this paper has established the rigorous mathematics model between FPCS and GCS, where the geocentric angle is computed. Furthermore, it has put forward the YAV calculation method. Simulation experiments give the trajectories width, and also analized the width changing at different latitudes and roll angles.

REFERENCES

[1] Cody, A., Denis, N., Andreas, B., and Michael, T., "Radiometric correction of RapidEye Imagery Using the on-orbit Side-slither Method", SPIE 8180, Image and Signal Processing for Remote Sensing XVII, 818008 , October 27, 2011.

[2] Corsini, G, Diani, M and Walzel, T., "Striping Removal in MOS-B Data." IEEE Transactions on Geoscience and Remote Sensing, 38(3):1439-1446, 2000.

[3] Gadallah, F.L., Csillag, F. Smith, E.J.M., "Destriping Multi sensor Imagery with Moment Matching," International Journal of Remote Sensing, 21, 2505-2511, 2000.

[4] Greslou D,Lussy Francoise de, Delvit,J.M., "PLEIADES-HR Innovative Techniques for geometric image quality commissioning," International Archives of the Photogrammetry, Remote Sensing and Spatial Information Sciences, Volume XXXIX-B1, 2012.

[5] Horn, B.K.P., Woodham, R.J., "Destriping Landsat MSS images by histogram modification," Computer Graphics and Image Processing, 10,69-83, 1979.

[6] Markham, B.L.,Schafer, J.S., etc, "Monitoring large-aperture spherical integrating sources with a portable radiometer during satellite instrument calibration," Metrologia, 35:643-648, 1998.

[7] Wang J.Q., Yu P,Yan C.X.,etc, "Space Optical Remote Sensor Image Motion Velocity Vector Computational Modeling, Error Budget and Synthesis," Chinese Optics Letters, 3(7), 414-417, July 2005.

Haichao Li was born in Shandong, China, in August 1979. He received the Dr. degree in Beijing University of Aeronautics and Astronautics.

He is currently an Associate Researcher of Qian Xuesen Laboratory of Space Technology. His main research interests are remote sensing, image and video processing, satellite calibration, stereo vision and navigation.

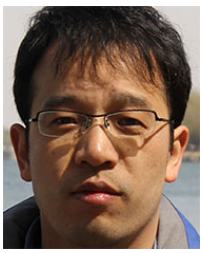

Yiyun Man was born in Hunan, China, in 1978. He received his Dr. degree in China Academy of Space Technology.

He is now an Associate Researcher. His research interests are remote sensing, image processing and restoration.